Monomer activity solely induces collapse of polymer chain in a good solvent

Aleksandr Buglakov [1,2,*] ,Vasilisa Lelecova [1,2], Aleksandr Chertovich [1,2]

1. Semenov Federal Research Center for Chemical Physics, Kosygina, 4, 119991 Moscow, Russia
2. Lomonosov Moscow State University, Leninskie gory 1, 119991 Moscow, Russia

*corresponding author's e-mail: buglakov@polly.phys.msu.ru

Abstract

Ability of particles to transform absorbed energy into translational movements brings peculiar orderings into the nonequilibrium matter. Connected together into the chain, these particles collectively behave completely different from well-known equilibrium polymers. Interestingly, one can find examples of active chains within cells. It is now proposed that activity, induced by molecular motor proteins play a key role in packing of chromatin within the cell nucleus.

Here we demonstrate the ability of the self-propulsion monomer units to cause polymer collapse under conditions where there is no explicit attraction between particles. The resulting conformation is heterogeneous and is characterized by a dense condensed core surrounded by elongated loops. The polymer segments in the condense phase have crumpled packing. Using molecular dynamics analysis, we show that this effect is similar to well-known motility induced phase separation, but more pronounced in active chains due to the polymers lack of entropy.

Introduction

Active matter is a new and rapidly developing field of modern nonequilibrium physics, with elements of biology and chemistry, partly explaining the unusual self-ordering observed in nature, including such phenomena as flocks of birds and colonies of bacteria [1,2]. Such environments consist of a sufficiently large number of interacting “active agents” that can convert internal energy or the energy of the environment into independent movement. It has been shown that, at a certain density and activity, such systems undergo motility-induced phase separation (MIPS), where part of the particles condenses and others exist within a gas-like state [3-6]. The reason for this ordering is a tendency of self-propelled particles to accumulate where their velocity decreases leading to effective attraction. This brings unusual phenomena to an existence - phase behavior of non-equilibrium active systems is strongly influenced by the translational and rotational inertia of active agents [7,8], in contrast to classical van der Waals phase diagrams [9].

In this context, it is intriguing to study the behavior of active polymers - chains of linearly bonded active agents. On the one hand, polymers are low in entropy and therefore easily self-assemble into sophisticated structures - almost all complex biological systems are of a polymeric nature. On the other hand several characteristic spatial scales could arise within a single macromolecule [10,11], that brings more complexity and sensitivity of polymer structures to the wide range of different signals.

Biologically relevant examples of active chains are microtubules and actin filaments - supramolecular polymers whose behavior within a cell is regulated through ATP consumption [12,13]. The substance of chromatin in the nuclei of eukaryotes and its morphology with division into euchromatin and heterochromatin can also be an example of self-organization of an active polymer [14,15]. Many attempts presented in the literature to describe the complex behavior of such systems within the framework of equilibrium processes are not convincing enough and a general consensus is yet to be obtained [16-20]. At that point the concept of active polymer as a model of biologically relevant nonequilibrium complexes is a good shot to bring better understanding into several sophisticated fundamental problems [22-24].

Recently, several works on active polymers, both on single chains and on interacting ensembles of many chains, have already appeared in the literature [25-36]. In ensembles of chains with different activities, a separation between active and passive chains were observed within two temperature models [34-36], generally similar to the behavior of low-molecular-weight active agents. Researchers of single chains noted stretching of polymer segments under the influence of activity [28-30], the chains demonstrate additional swelling starting from some fairly high activity. A few studies noted the effect of coil's small shrinking before the activity-induced swelling [30-32], which the authors associated with the local ordering of chain segments in a zig-zag conformation. It has been suggested that the mechanism of polymer compression is somehow related to MIPS [31], but to further develop this idea it is necessary to observe a stable condense state within a single chain, that is, increase the tendency of the monomer units to effectively attract each other without bringing explicit attraction potentials.

In this work, we demonstrate for the first time that single polymer chains in a good solvent can collapse into a condensed state under the influence of the activity of monomer units. This effect is observed in a narrow range of intermediate activities, and for fairly long polymer chains. Moreover, this collapsed state is not a classical globule; it is loose and heterogeneous, exhibiting separation into stretched and dense regions. In summary, we showed that activity alone can control the conformational behavior of polymer coils, ranging from collapsed conformations to swollen coils.

Results

Let us consider single homopolymer chains in the good solvent regime. Of the interactions, we will leave only the excluded volume - strong repulsion when monomer units overlap; the modeling details are given below in the methods section. In this regime, a chain of length N is in the form of a swollen coil with a scaling size, which we will traditionally describe using the radius of gyration Rg, Rg ~ $N^{3/5}$. Now, the question is - how polymer conformation would be affected by the introduction of self-propulsion to every monomer unit independently, given that equations of motion include both translational and rotational inertia. Thus, we consider a chain of active brownian particles in an underdamped regime [7] with m - mass of the particles and J - moment of inertia (for details see Methods).

We will study the behavior of such a system as activity increases. Here, parameterization of activity is done using the dimensionless Peclet number parameter Pe = vσ/D, where v - active velocity, σ - diameter of the monomer units and D - translational diffusion coefficient. This parameter describes the ratio between activity-induced diffusion and classical temperature dependent one (more strictly - ratio between characteristic times of rotational and translational diffusion). The main result is presented in Figure 1a. For relatively short chains, for example for N=256, at a certain critical value Pe ≈ 15, a transition to an even more swollen state occurs. This transition is caused by an effective stiffening of the chain, an apparent increase in persistence length and has previously been described, see for example [26], but for a slightly different set of model parameters, and therefore a different critical value of Pe. The same work noted a slight shrinking before swelling, which the authors attributed to the formation of zigzag conformations near the transition.

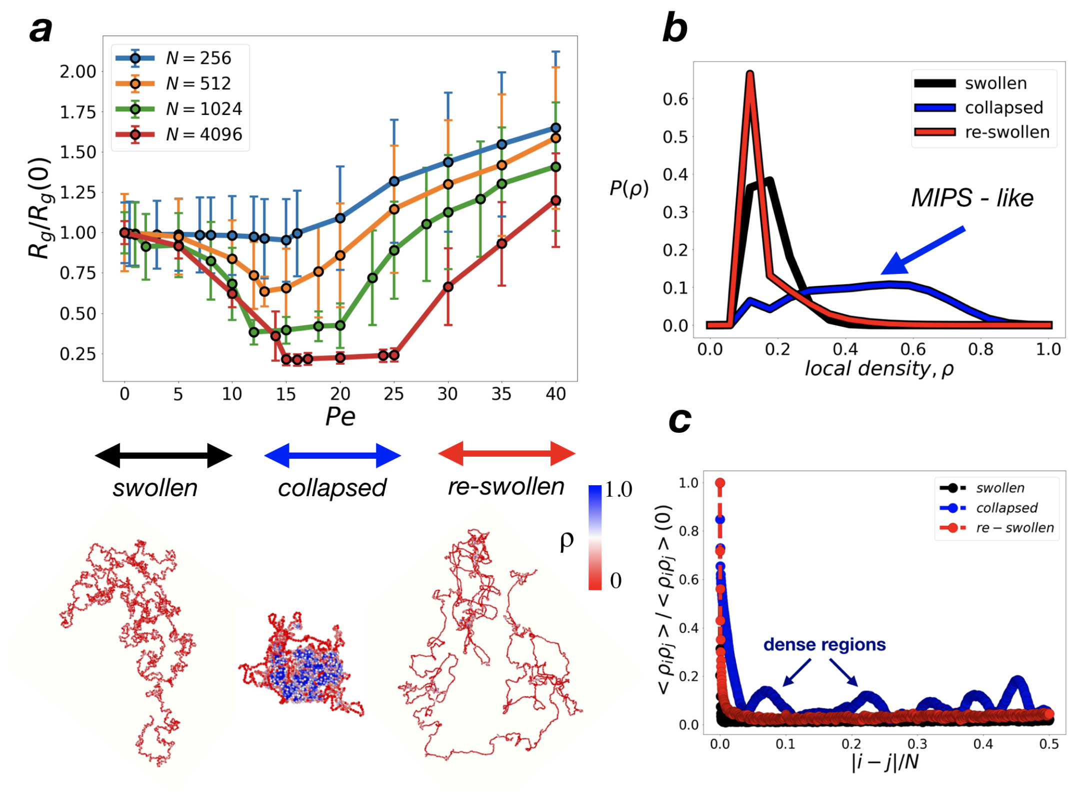

Figure 1. Dependence of normalized gyration radius R_g on Pe for active polymers of different polymerization degree N with instant snapshots of active polymers typical conformations with N = 4096 at different Pe (a); Coordination numbers distributions for different chain states (b); normalized correlation function $<\rho_i\rho_j>$ of coordination numbers along the chain (c).

However, if we start increasing the length of the chains in question, the situation changes drastically. As the degree of polymerization increases, an increasingly deeper and wider minimum appears at intermediate Pe; we can talk about the observation of the collapse phenomenon. For the degree of polymerization N = 4096, one can clearly observe the presence of some stable region of the collapsed conformation; in the range $15 < Pe < 25$, the radius of gyration is only 25% of the unperturbed swollen coil. Activity-induced collapse of the chain of self-propelled monomer units is followed by polymer re-swelling at high-enough Pe.

Thus, one can divide an observable set of active polymer conformations into three distinct types. Typical snapshots of these states for the $N = 4096$ are shown in Figure 1a with monomer units colored by their local density ρ. At low Pe polymer in a swollen state, where conformation is primarily determined by excluded volume of the monomers units. Intermediate Pe renders the collapsed state of the macromolecule with clearly visible separation onto dense regions and stretched loop fragments. Third state occurs at high Pe - there are alternations of highly stretched fragments with small collapsed blobs.

Two competing effects - stretching and activity-induced condensation determines chain size and conformation as a whole. On the one hand, connectivity brings a unique process into the system - local stretching. On the other - stretched segments can act as active agents themselves, with the ability to aggregate. We claim that the collapsed state of the long active polymer chain occurs within the same physical reasons as MIPS in active gas [6], but at lower Pe due to intrinsically low translational entropy of monomer units. For comparison, we carried out several test calculations in a gas system with $N = 1$ and showed that at a similar density, MIPS is not observed; in order for MIPS to appear, both the concentration and Pe must be significantly increased - we observed separation at Pe=300 and concentration $N/V = 0.5$ (see SI1). Connectivity of active particles provides higher collision probability and increases spatial correlation time between monomer units.

Similarity between MIPS of active gas system and collapse of active polymer arises as the appearance of bimodal distribution of monomer units local density in the collapsed state (Figure 1b blue curve). Here, one small peak at low density stands for freely moving stretched fragments - there are only two neighbors in the vicinity of each monomer unit. Second wide peak at higher densities describes the presence of dense regions, separated from stretched ones. As the chain enters a re-swollen state, the second peak disappears and the first peak of monomer units in stretched regions becomes dominant.

Another feature of collapsed conformation of active polymer is a continuous correlation of local monomer unit densities along the chain (Figure 1c). In the contrast to swollen and re-swollen state, collapsed polymer exhibits undamped correlation, expressed in appearance of alternates local peaks of normalized $\langle \rho_i \rho_j \rangle$ along the chain, which indicate presence of alternates loops, surrounding single dense region. Here, the chain as whole highly shrinked, however stretched segments form several loops on the surface of a globule. Thus, the initial homopolymer sequence becomes fragmented into two types of blocks - stretched blocks and collapsed ones.

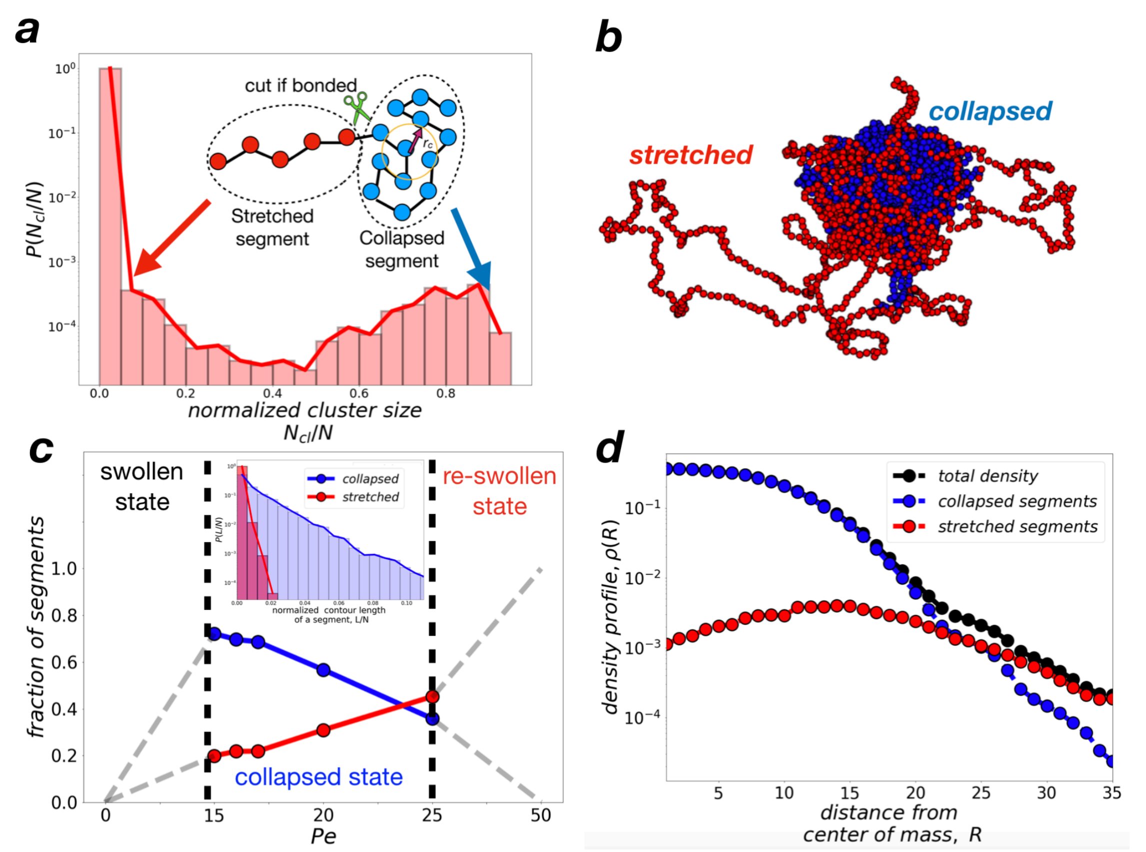

Figure 2. Aggregation number distribution for collapsed chain (a); ; instant snapshots of active chain conformations within the R_g minima at $Pe = 15$ with collapsed segments colored blue and stretched segments colored red (b); Fraction of collapsed (blue) and stretched (red) segments depending on Pe in the collapsed polymer state at N = 4096. Dashed line indicates probable values for swollen and re-swollen states. Inset shows distributions of stretched and collapsed segments contour length for collapsed chain with Pe = 15 (*c*); normalized radial density profile of the collapsed and stretched segments for collapsed chain (d).

We established that activity can induce collapse of the long-enough polymer chain and observed separation within the collapsed state on dense and stretched loop regions. Now, let us dive into features of these separated regions. Cluster analysis was employed to distinguish two different types of fragments within a single polymer (see Methods). Figure 2a shows distribution of normalized aggregation numbers N_{cl}/N for the collapsed state. As one can see there are two pronounced peaks - one of cutted monomer units in stretched loops and other of single large clusters of condensed monomer units. Second maxima occurs at ~ 0.8 as most of the monomer units are part of this large cluster. In a collapsed polymer state there are large single clusters and stretched chain fragments. From now on, for the sake of certainty we will call continuous low density segments - stretched segments and chain parts within a condensed state - collapsed segments. Typical conformation of collapsed chain with monomer units colored depending on belonging to one or other type shown in Figure 2b.

As was shown above, there is alternation between stretched and collapsed segments along the chain. Average fraction of collapsed segments for the N = 4096 on most of the collapsed state Pe intervals is larger than the fraction of stretched segments (Figure 2c). Crossover point where this ratio reverses indicates the starting point of chain reswelling. Within the collapsed chain typical length of the latter segments is significantly larger than of the former ones. At the same time, length distributions of both segment types are Flory-like (exponential), and no characteristic segment size can be observed. Interestingly, two types of segments form core-shell-like arrangement within collapsed conformation, where core is rather formed by collapsed segments and stretched ones tend to locate in the exterior of the structure as confirmed through radial density profile (Figure 2d). Note, due to strong asphericity of collapsed conformation observed radial density profile distinct from analogues profile for block-copolymer micelles, where fraction of solvophilic blocks drops to zero in the core bulk [37].

Let us further consider the structure properties of collapsed and stretched segments separately. Figure 3a shows the dependence of the root-mean-square distance in space on the distance along the chain R(s), as well as the probability of contact on the distance along the chain P(s) (Figure 3b) for the different segments, swollen, re-swollen and globular states. The stretched segments have a significantly greater persistent length than the swollen coil at Pe=0, but at s ~ 20 there is small local minima, corresponding to formation of loop for on the surface of the collapsed conformation P(s) dependence renders more pronounced evidence of loop formation - there is clear maxima of P(s) at s = 20 for stretched segments - overall its double folded stretched fragment.

The collapsed regions at short s are also stretched. At s ~ 10 there is nonmonotonic change in the derivative, corresponding to local crumpling of the segments. Formation of crumples along the chains is also confirmed by P(s) dependence, with pronounced maxima at s = 10. At s > 10 collapsed segments have scaling 0.44, which is close but slightly lower then ideal packing according to Flory's theorem [38]. For the sake of clarity, R(s) and P(s) for classical globule are also shown in Figure 3a-b. Note the connection between the observed dependencies and the fractal globule and recent studies of chromatin structure [39]. As in these works, we observe folding that characterizes some intermediate state between the equilibrium “gaussian” conformation with scaling 1/2 and the ideal fractal structure (Hilbert curve) with scaling 1/3.

For the re-swollen chain there are two regimes of R(s) and P(s) - large stretching is followed by ½ and -1.5 regime correspondingly, showing that at high Pe this confirmation could be described as random walk of large stiff segments. Gaussian scaling arises as under collisions effective excluded volume could decrease - stiff segments may bend in a collision, unlike in the case of a true rigid-chain polymer.

One of the possible explanations for the specific folding of the collapsed segments lies in its dynamics, fundamentally nonequilibrium nature, due to the constant elongation of new loops and the collapse of old ones, and the hindered redistribution of monomer units between collapsed and elongated segments (Figure 3c). Let us recall that in our homopolymer model all monomer units are identical in interactions and therefore membership in collapsed state or elongated segment is determined stochastically, virtually randomly, and can be changed at a random point in time. Mixing between two types of segments was estimated through function $I = A \cdot < (\frac{N_b - <N_{cl}>}{N})^2 >$, where N_b - average cluster size of the largest cluster, N - polymerization degree, A- normalization constant (I(0) = 1; I(inf) = 0); It’s seen that the rate of mixing between initially marked stretched and collapsed segments increases with Pe (Figure 3d). Similar to MIPS in active gas, collapsed segments are trapped within the condensed region and move slowly, which hinders relaxation to ideal globular scaling.

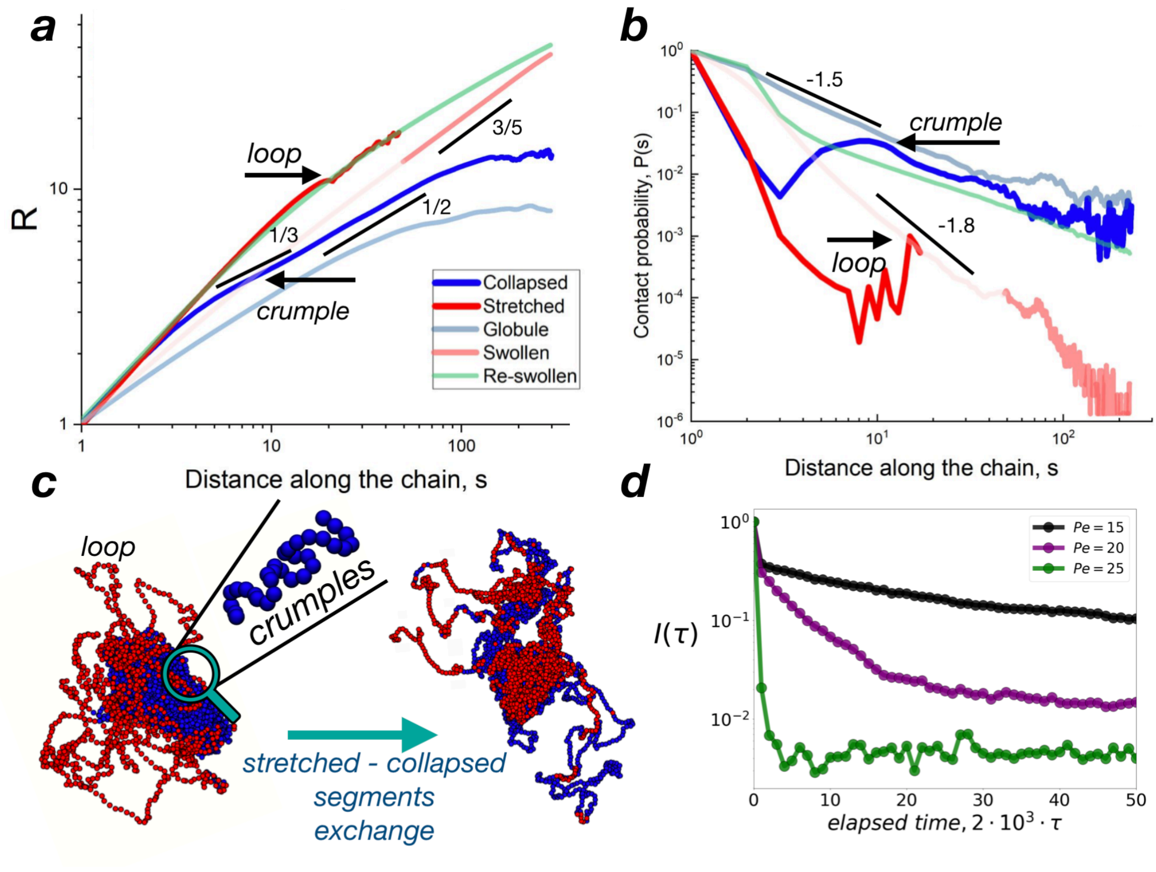

Figure 3. Distance between monomers R on contour distance along the chain s for different chain conformations (a); Contact probability P on contour distance along the chain s for different chain conformations (b); Illustration of monomer exchange between two separated states in time (c); Monomer mixing function $I(t)$ between stretched and collapsed state depending on elapsed time (d);

Finally, let's look at how sensitive the observed phenomena are to the choice of model parameters, in particular rotational and translational inertia, introduced through parameters J and m; see methods section for details. These two parameters, which at first glance are not particularly important for equilibrium properties, can play a decisive role when considering nonequilibrium systems with activity [7-8]. Translational inertia has the meaning of mass, and rotational inertia in a sense describes the asymmetry of the motion of a single particle. Importantly, introduction of rotational inertia induces large decorrelation time of velocity direction, reducing effective rotational diffusion. At the same time activity promotes local stretching of the chains - the effect that is obviously absent in the active gas.

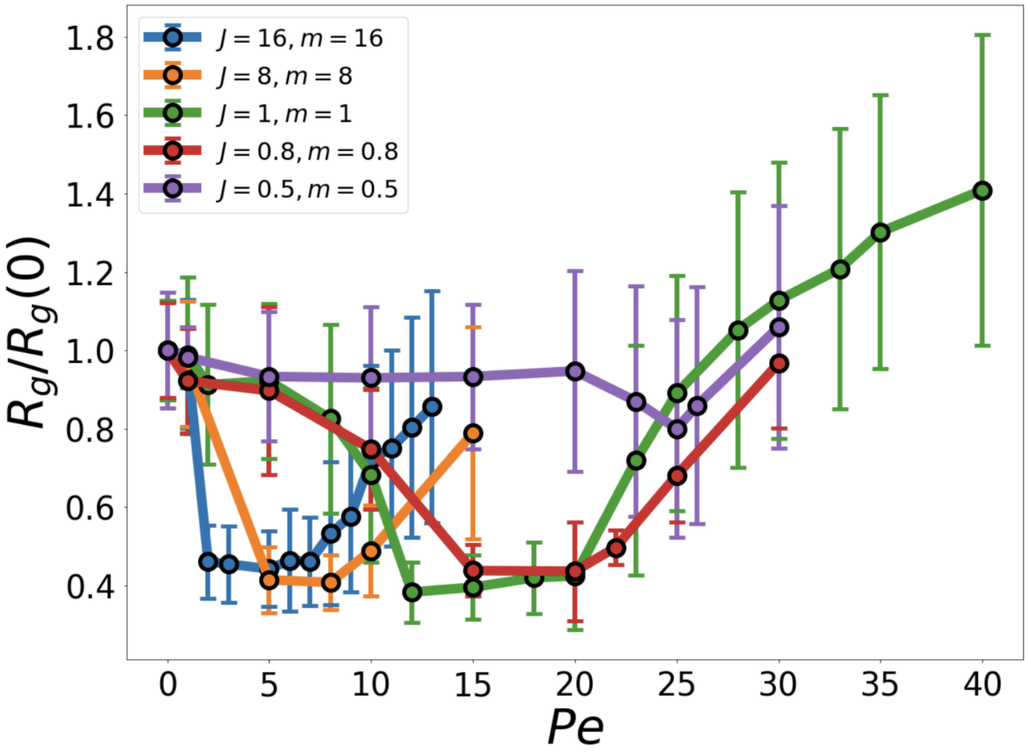

Figure 4. Rg dependence of active chain with $N = 1024$ on Pe at different J and m with $J/m = 1$.

We calculated Rg dependencies on Pe at different J and m keeping constant ratio $J/m = 1$. Curves for the chain of length $N = 1024$ are shown in Fig. 5. Despite $J/m = 1$ for every dependency, they strongly differ, as for large $J = 16$ and $m = 16$ collapse occurs at lower Pe compared to other J and m considered. One can see that increase in absolute values of inertia terms leads to a curve shift towards larger Pe. Interestingly, for the lowest of considered J and m region of minima not only shifts toward higher activity degree, but has significantly lower depth. There is no surprise, as with J and m approaches 0, equation of motions transforms into classical ABP equations in overdamped regime, where only slight chain size decrease at intermediate Pe was observed.

Importantly, observed phenomena are steady within nonequilibrium dynamics and are observed within a wide range of parameters. We suggest that collapse of the active polymer chain is a universal effect that can be observed in different activity models at some large polymerization degree.

Conclusions

We demonstrated for the first time the possibility of single homopolymer chain collapse upon exposure to activity alone. At some intermediate values of activity, a chain of a large number of monomers collapses into a much denser state than a swollen coil. Moreover, this state is heterogeneous, some of the monomer units form elongated segments, some are collapsed, and as activity increases, the ratio changes in favor of more elongated ones.

In fact, we demonstrated that interactions between monomer units can be controlled via activity. Once a transition to a collapsed state is observed for a single chain, then for a system of overlapping coils, block copolymers and other interacting polymer systems - all of them will also be subject to conformational and morphological changes under the influence of activity. We believe that such control by activity can play an important role when considering various biological systems, the understanding and description of which is not yet possible using the methods of classical equilibrium thermodynamics.

Methods

Active polymer chain is modeled as a set of N beads with diameter σ connected through harmonic bonds of equilibrium length l. Activity is introduced via force $f^a = nv_a$ within active brownian particle (ABP) concept, where v_a is active velocity defining amplitude of the force and n - orientation unit vector. In ABP variation of f^a orientation n is determined by random torque, acting stochastically on every active particle independently. The Langevin equation defines translational motion of monomers. In contrast to the classical ABP model, where inertia force terms are neglected, here we keep them in both translational and rotational equations [7], hence, underdamped dynamics is realized in our simulations. Equation of motion can be written as:

$$m v_i' = -\gamma v_i + F_i + \sqrt{2T\gamma}\xi_i + f_i^a \quad (1)$$

$$J\omega_i' = -\gamma\omega_i + \gamma\sqrt{2D_r}\eta_i \quad (2)$$

where v_i and ω_i are translational and angular velocities of particle i; m and J are mass and moment of inertia, γ is friction coefficient, T - temperature. D_r is rotational diffusion coefficient related to translational diffusion coefficient D_t as $D_r = 3D_t/\sigma$. F_i is a particle's interaction force, acting on current particle i. In our case there are only two types of particle-particle interactions: Weeks-Chandler-Andersen potential [40] which is cutted and shifted to minima position LJ potential $U = 3\epsilon\left[(\sigma/r)^{12} - (\sigma/r)^{6}\right]$ - this potential is utilized to bring excluded volume interactions and thus exert thermodynamically good solvent statistics of the passive ($f^a = 0$) polymer; Harmonic bond interaction $U = \frac{1}{2}k\left(r_{i,i+1} - l\right)^2$ with equilibrium bond length $l = 1$ and stiffness $k = 10^3$ which brings connectivity between monomer units. ξ and η_i are gaussian white-noise terms. Temperature of the langevin thermostat was set as $T= 1$, friction coefficient $\gamma = 1$, translational diffusion coefficient $D = 1$.

Strength of activity was characterized by dimensionless Peclet number $\mathrm{Pe} = |f^a|\sigma/D_r = v_{a\sigma}/3D$ and was changed through variation active force amplitude v_a. Within this work we were particularly interested in regions of possible chain shrinkage at intermediate activity, so large Pe at which high elongation of the polymer occurs were mostly neglected. We addressed rotational and translational inertia effects on active polymer chain conformation, so both m and J were varied in the range [0.5,16]. Simulations were carried out with LAMMPS [41] open-source package with in-house modified code. Integration step of each simulation was set as $dt = 5 \times 10^{-4}$. Each relaxation run was conducted within enough number of timesteps N_{dt} to ensure conversion of gyration radius of the chain $<R_g>$ provided that N_{dt} much greater than average time of the chain diffusion through simulation box $L = 300$, $N_{dt} = 2 \times 10^9$ timesteps.

Classical algorithm of clusterization [42] was utilized with cut-off distance $r_c = 1.5\ \sigma$ to separate monomers in condensed state from monomers in stretched loops with simple modification - bonded particles were excluded from neighbors and two connected monomers i and i+1 could be found in the single cluster only if there is a path between them through other neighbors.

Acknowledgments

The work was done within the framework of the Russian Science Foundation Project No. 23-73-00089. This research was carried out using the equipment of the shared research facilities of HPC computing resources at Lomonosov Moscow State University.

DATA AVAILABILITY

All presented and analyzed data is included in both main text and in the Supplementary Material, including the methods and force fields. Additional data, including simulations scripts, that support the findings of this study are available from the corresponding author upon reasonable request.

AUTHOR DECLARATIONS Conflict of Interest

The authors have no conflicts to disclose.

References:

[1] Shaebani, M. R., Wysocki, A., Winkler, R. G., Gompper, G., & Rieger, H. . Computational models for active matter. Nature Reviews Physics, **2**, 181-199 (2020).

[2] Needleman, D., & Dogic, Z. Active matter at the interface between materials science and cell biology. Nature reviews materials, **2**, 1-14 (2017).

[3] Cates, M. E., & Tailleur, J. Motility-induced phase separation. Annu. Rev. Condens. Matter Phys., **6,** 219-244 (2015).

[4] Caporusso, C. B., Digregorio, P., Levis, D., Cugliandolo, L. F., & Gonnella, G. Motility-induced microphase and macrophase separation in a two-dimensional active Brownian particle system. Physical Review Letters, **125**, 178004 (2020).

[5] Stenhammar, J. An Introduction to Motility-Induced Phase Separation. arXiv preprint arXiv:2112.05024 (2021).

[6] Stenhammar, J., Tiribocchi, A., Allen, R. J., Marenduzzo, D., & Cates, M. E. Continuum theory of phase separation kinetics for active Brownian particles. Physical review letters, **111,** 145702 (2013).

[7] Caprini, L., Gupta, R. K., & Löwen, H. Role of rotational inertia for collective phenomena in active matter. Physical Chemistry Chemical Physics, **24,** 24910-24916 (2022).

[8] Scholz, C., Jahanshahi, S., Ldov, A., & Löwen, H. Inertial delay of self-propelled particles. Nature communications, **9,** 5156 (2018).

[9] Chandler, D., Weeks, J. D., & Andersen, H. C. Van der Waals picture of liquids, solids, and phase transformations. Science, **220,** 787-794 (1983).

[10] De Gennes, P. G. Scaling concepts in polymer physics (Cornell university press. 1979).

[11] Stuart, M. A. C., et al. Emerging applications of stimuli-responsive polymer materials. Nature materials, **9,** 101-113 (2010).

[12] Budaitis, B. G., et al. A kinesin-1 variant reveals motor-induced microtubule damage in cells. Curr. Biol. **32,** 2416–2429.E6 (2022).

[13] Weber, C. A. Random bursts determine dynamics of active filaments. Proc. Natl. Acad. Sci. U. S. A. **112,** 10703–10707 (2015).

[14] Mahajan, A., Yan, W., Zidovska, A., Saintillan, D., Shelley, M. J. Euchromatin activity enhances segregation and compaction of heterochromatin in the cell nucleus. Phys. Rev. X **12,** 041033 (2022).

[15] Weber, S. C., Spakowitz, A. J., Theriot, J. A. Nonthermal ATP-dependent fluctuations contribute to the in vivo motion of chromosomal loci. Proc. Natl. Acad. Sci. U. S. A. **109,** 7338–7343 (2012).

[16] C. Nguyen, et al. Emergent collective locomotion in an active polymer model of entangled worm blobs. Front. Phys. **9,** 734499 (2021).

[17] Gavrilov, A. A., et al. Unraveling the mechanisms of chromatin fibril packaging. Nucleus, **7,** 319-324 (2016).

[18] Ulianov, S. V., et al. Active chromatin and transcription play a key role in chromosome partitioning into topologically associating domains. Genome research, **26,** 70-84 (2016)..

[19] Mirny, L. A. The fractal globule as a model of chromatin architecture in the cell. Chromosome research, **19,** 37-51 (2011).

[20] Ulianov, S. V., et al. Nuclear lamina integrity is required for proper spatial organization of chromatin in Drosophila. Nature communications, **10,** 1176 (2019).

[21] Conte, M., et al. Polymer physics indicates chromatin folding variability across single-cells results from state degeneracy in phase separation. Nature communications, **11,** 3289 (2020)..

[22] Bruinsma, R., Grosberg, A. Y., Rabin, Y., & Zidovska, A. Chromatin hydrodynamics. Biophysical journal, **106,** 1871-1881 (2014).

[23] Eshghi, I., Zidovska, A., & Grosberg, A. Y. Activity-driven phase transition causes coherent flows of chromatin. Physical Review Letters, **131,** 048401 (2023).

[24] Goychuk, A., Kannan, D., Chakraborty, A. K., & Kardar, M. Polymer folding through active processes recreates features of genome organization. Proceedings of the National Academy of Sciences, **120,** e2221726120 (2023).

[25] Vutukuri, H. R., Bet, B., Van Roij, R., Dijkstra, M., & Huck, W. T. Rational design and dynamics of self-propelled colloidal bead chains: from rotators to flagella. Scientific reports, **7,** 16758 (2017).

[26] Kaiser, A., Babel, S., ten Hagen, B., von Ferber, C., & Löwen, H. How does a flexible chain of active particles swell?. The Journal of chemical physics, **142,** (2015).

[27] Duman, Ö., Isele-Holder, R. E., Elgeti, J., & Gompper, G. Collective dynamics of self-propelled semiflexible filaments. Soft matter, **14,** 4483-4494 (2018).

[28] Isele-Holder, R. E., Elgeti, J., & Gompper, G. Self-propelled worm-like filaments: spontaneous spiral formation, structure, and dynamics. Soft matter, **11,** 7181-7190 (2015).

[29] Li, H. S., Zhang, B. K., Li, J., Tian, W. D., & Chen, K. Brush in the bath of active particles: Anomalous stretching of chains and distribution of particles. The Journal of chemical physics, **143,** (2015).

[30] Martín-Gómez, A., Eisenstecken, T., Gompper, G., & Winkler, R. G. Active Brownian filaments with hydrodynamic interactions: Conformations and dynamics. Soft matter, **15,** 3957-3969 (2019).

[31] Das, S., Kennedy, N., & Cacciuto, A. The coil–globule transition in self-avoiding active polymers. Soft Matter, **17,** 160-164 (2021).

[32] Vatin, M., Kundu, S., & Locatelli, E. Conformation and dynamics of partially active linear polymers. Soft Matter, **20,** 1892-1904 (2024).

[33] Rudyak, V. Y., Lopushenko, A., Palyulin, V. V., & Chertovich, A. V. Long-range ordering of velocity-aligned active polymers. The Journal of Chemical Physics, **160,** (2024).

[34] Smrek, J., Chubak, I., Likos, C. N., & Kremer, K. Active topological glass. Nature communications, **11,** 26. (2020).

[35] Chubak, I., Pachong, S. M., Kremer, K., Likos, C. N., & Smrek, J. Active Topological Glass Confined within a Spherical Cavity. Macromolecules, **55,** 956-964 (2022).

[36] Smrek, J., & Kremer, K. Interfacial properties of active-passive polymer mixtures. Entropy, **20,** 520 (2018).

[37] Milchev, A., Bhattacharya, A., & Binder, K. Formation of block copolymer micelles in solution: A Monte Carlo study of chain length dependence. Macromolecules, **34,** 1881-1893 (2001).

[38] Khokhlov, A. R., Grosberg, A. Y., & Pande, V. S. Statistical physics of macromolecules (Vol. 1) (New York: AIP press, 1994).

[39] Tamm, M. V., Nazarov, L. I., Gavrilov, A. A., & Chertovich, A. V. Anomalous diffusion in fractal globules. Physical review letters, **114,** 178102 (2015).

[40] Weeks, J. D., Chandler, D., & Andersen, H. C. Role of repulsive forces in determining the equilibrium structure of simple liquids. The Journal of chemical physics, **54,** 5237-5247 (1971).

[41] Thompson, A. P., et al. LAMMPS-a flexible simulation tool for particle-based materials modeling at the atomic, meso, and continuum scales. Computer Physics Communications, **271,** 108171 (2022).

[42] Allen, M. P., & Tildesley, D. J. Computer simulation of liquids (Oxford university press., 2017).

Author Information

Authors and Affiliations

Semenov Federal Research Center for Chemical Physics, Kosygina, 4, 119991 Moscow, Russia

Aleksandr Buglakov ,Vasilisa Lelecova, Aleksandr Chertovich

Lomonosov Moscow State University, Leninskie gory 1, 119991 Moscow, Russia

Aleksandr Buglakov , Vasilisa Lelecova, Aleksandr Chertovich,

Contributions

A.V., A.B. designed the research and parameterized the model, A.B. performed the simulations, A.B., V.L. and A.V. analyzed the data, A.B and A.V. wrote the paper.

Corresponding authors

Correspondence to Aleksandr Buglakov: buglakov@polly.phys.msu.ru

SUPPLEMENTARY INFORMATION

Monomer activity solely induces collapse of polymer chain in a good solvent

Aleksandr Buglakov [1,2,*] ,Vasilisa Lelecova [1,2], Aleksandr Chertovich [1,2]

1. Semenov Federal Research Center for Chemical Physics, Kosygina, 4, 119991 Moscow, Russia
2. Lomonosov Moscow State University, Leninskie gory 1, 119991 Moscow, Russia

*corresponding author's e-mail: buglakov@polly.phys.msu.ru

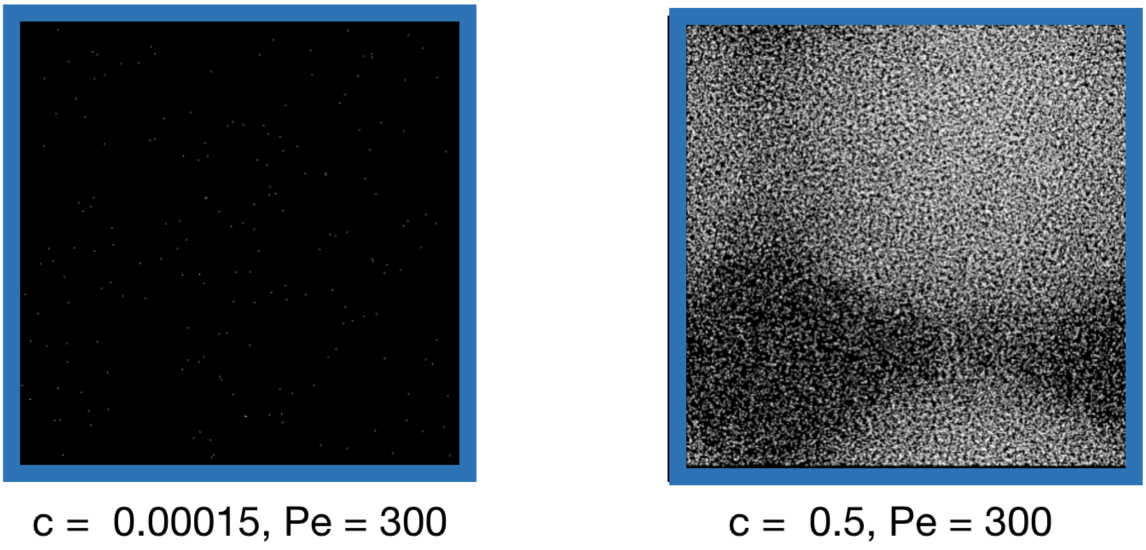

Supplementary Figure 1. Instant snapshots of active ABP particles system with *m* = 1 and *J* = 1 at concentration c = N/V = 0.00015 and c = 0.5 with Pe = 300. Left snapshot indicates the gas state, the right snapshot indicates separation between condensed and gas states. Both simulations performed at temperature T = 0.01 to exclude thermal fluctuation effects.